Science Advances
AAAS

Supplementary Materials for

Identification of a humanized mouse model for functional testing of immune-mediated biomaterial foreign body response

Joshua C. Doloff *et al.*

Corresponding author: Joshua C. Doloff, jcdoloff@jhu.edu; Dale L. Greiner, dale.greiner@umassmed.edu; Daniel G. Anderson, dgander@mit.edu

Sci. Adv. **9**, eade9488 (2023)
DOI: 10.1126/sciadv.ade9488

This PDF file includes:

1. Supplementary Figures:

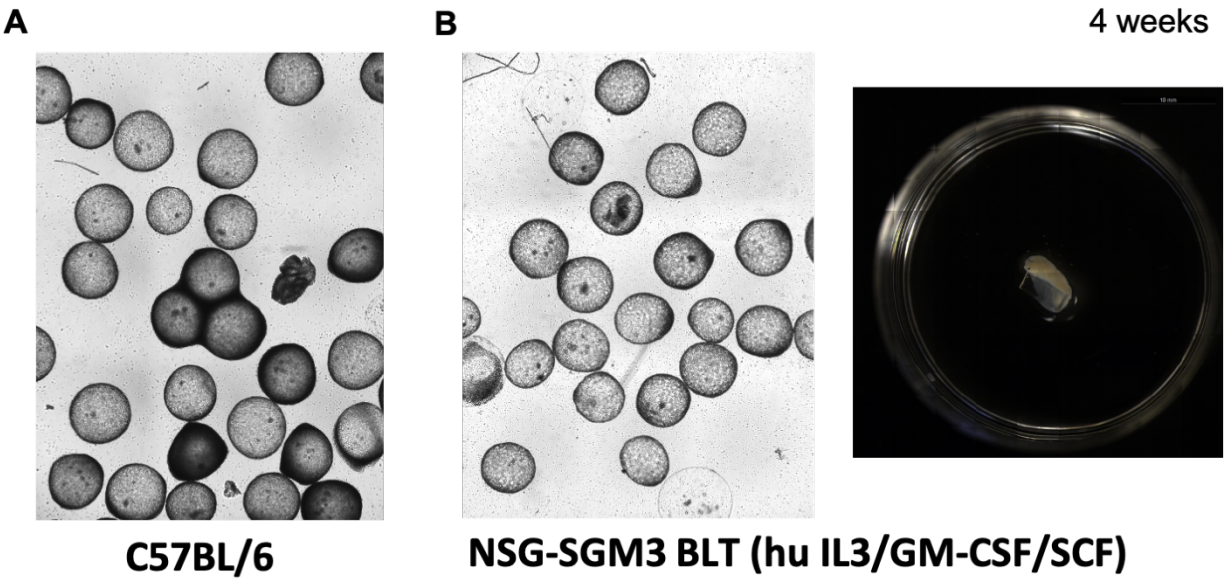

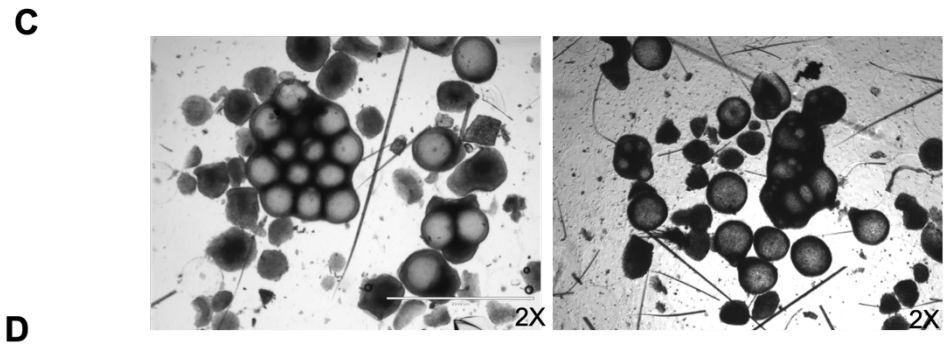

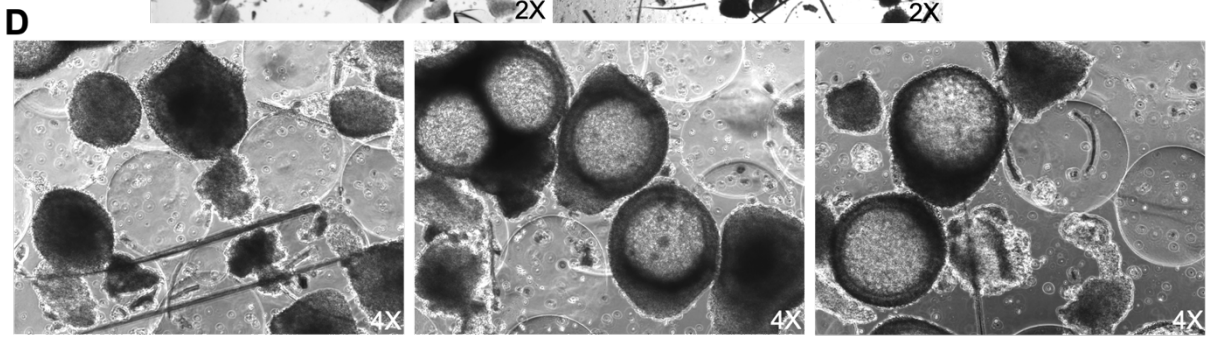

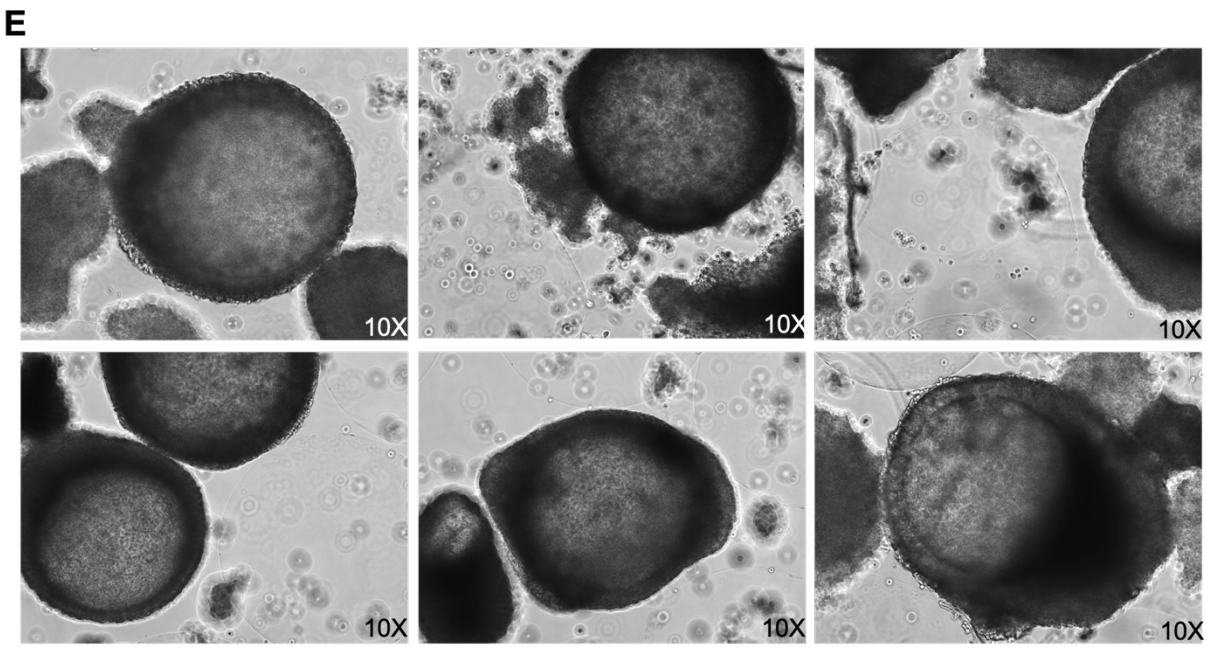

Supplemental Figure S1. Transgenic delivery of 3 Human cytokines (IL3, GM-CSF, and SCF) enabled fibrosis in the engrafted NSG-SGM3 BLT model. A) SLG20 alginate 500 μm diameter spheres were implanted into the intraperitoneal (IP) space of C57BL/6 mice, where they were retained for 14 days and analyzed upon retrieval. Both brightfield (left) as well as phase contrast imaging (right) is shown. **B)** Similar SLG20 spheres retrieved after 2- or 4-week IP implantations in the NSG-SGM3 BLT model (left: brightfield at 2 weeks; right: phase contrast at 4 weeks, with sample embedded in epididymal fat). Photos representative from n = 5 mice per treatment. **C-E**) Additional micrographs of retrieved fibrosed capsules at 2X, 4X, and 10X magnifications, respectively. Experiment run twice.

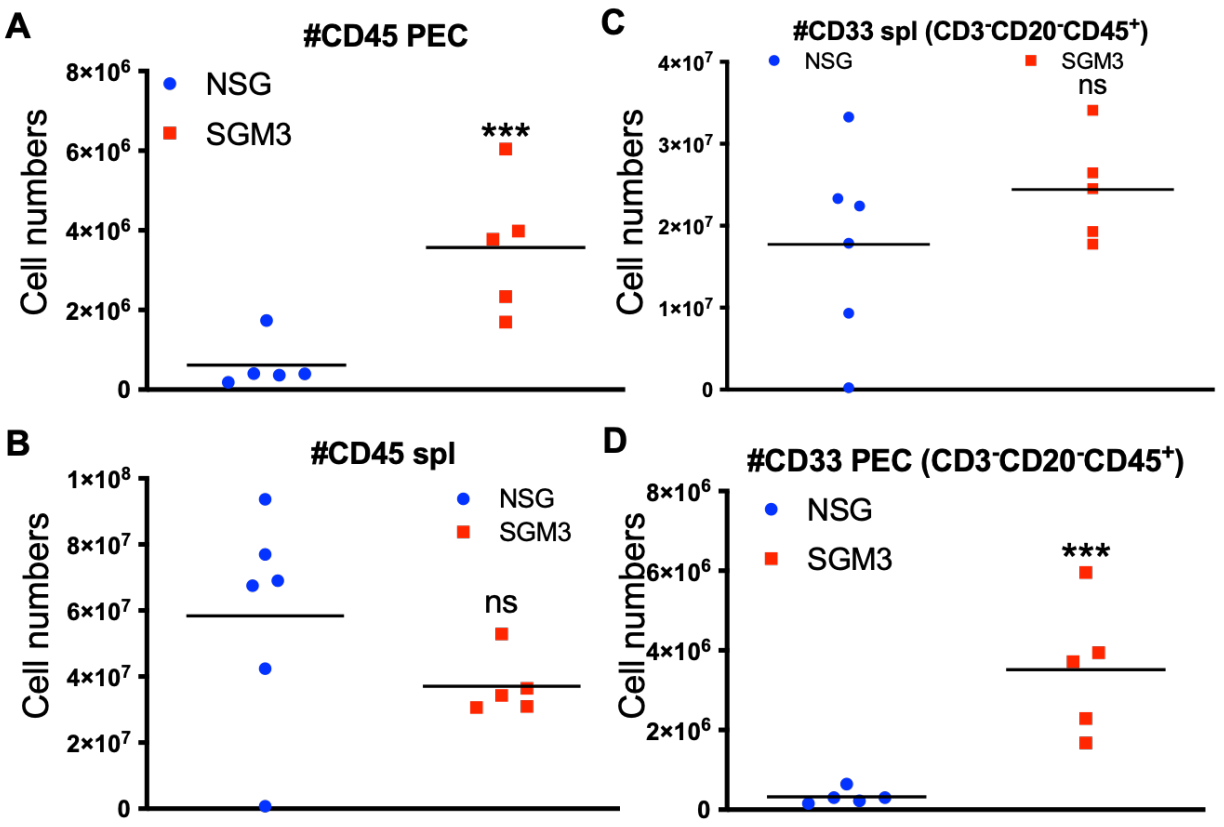

Supplemental Figure S2. SGM3 cytokine modification of humanized mice increased CD45$^+$ immune cells in the IP space, and innate myeloid CD33$^+$ immune cells in both the spleen and IP space of engrafted mice. A) Flow cytometry analysis of IP lavage peritoneal exudate cells (PEC) showed significant increases in human CD45$^+$ white blood cell numbers following SGM3 cytokine inclusion to support human immune engraftment in NSG-SGM3 BLT mice. **B)** While CD45$^+$ numbers were not significantly increased in spleens (spl) isolated and dissociated from NSG-SGM3 BLT engrafted mice (top), **C**) the fraction of CD33$^+$ (CD3$^-$CD20$^-$) cells were increased (bottom). **D)** Significant increases were observed for CD33$^+$ myeloid cells in peritoneal exudate from SGM3 engrafted mice. Lines, mean. All y-axes show absolute cell numbers (#). n = 5 mice per treatment. Performed two times.

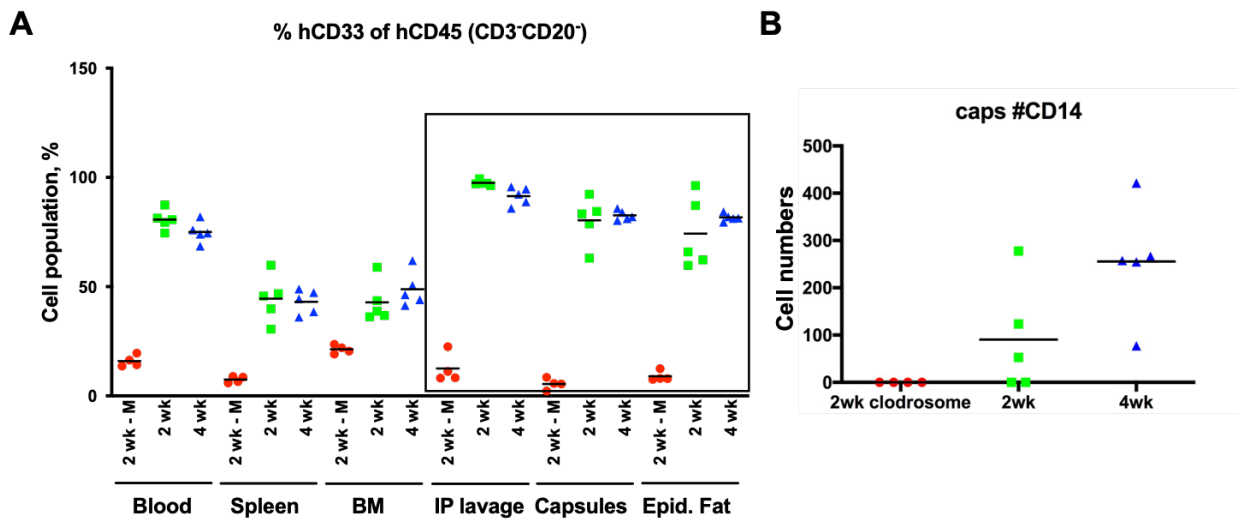

Supplemental Figure S3. SGM3 modification of engrafted humanized mice results in macrophage enrichment across multiple compartments of the intraperitoneal space. A) Flow cytometry (% composition) showing site-specific (intraperitoneal in IP lavage, from IP implanted capsules, or isolated epididymal fat) increases in mature human $CD45^{+}CD33^{+}CD3^{-}CD20^{-}$ myeloid macrophages over 2 or 4-week implantations (green and blue, respectively) versus reduced with clodrosome-maintained macrophage depletion at 14 days post-implant (red) in engrafted NSG-SGM3 BLT mice. **B)** Flow-based determination (cell numbers) of $CD45^{+}CD14^{+}$ monocytic infiltration at 2- and 4-weeks post-implant, with none following clodrosome depletion. n = 5 mice/group. The same material volume of hydrogel spheres was implanted into each mouse in all cases. Experiments were repeated twice.

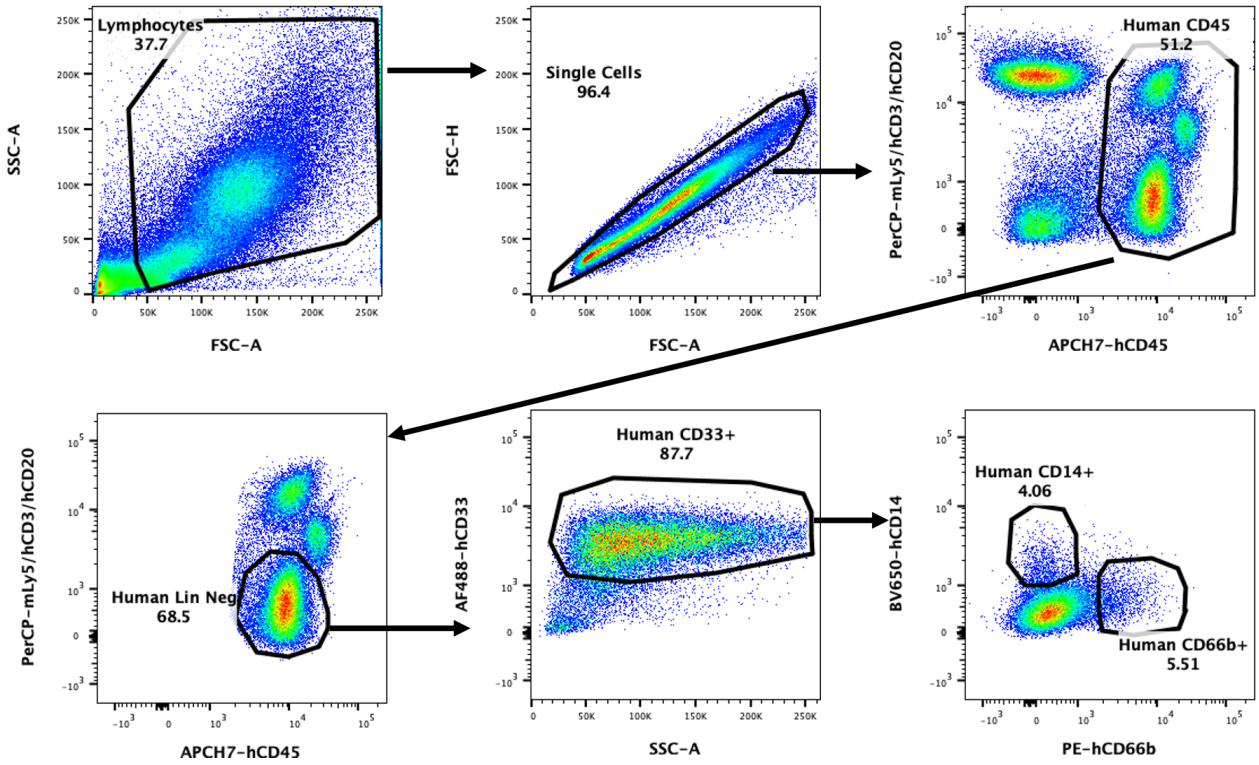

Supplemental Figure S4. Flow cytometry gating scheme for innate human immune cell populations isolated from engrafted NSG-SGM3 BLT mice. Flow cytometry analysis gating scheme for human immune cell markers (CD45, general leukocytes; CD33 ($CD3^-CD20^-$), myeloid lineage; CD14 (also $CD3^-CD20^-$), monocytes; and CD66b, neutrophils) analyzed in samples isolated from human immune engrafted NSG-SGM3 BLT mice. Note: CD33+ cells shown are also $CD3^-CD20^-$ (shown in the bottom left panel y-axis, 3 markers are utilized on the y-axis). Performed two times for blood, spleen, bone marrow, IP lavage, as well as dissociated epididymal fat or cells isolated from the surface of biomaterial implants. N = 5 mice.

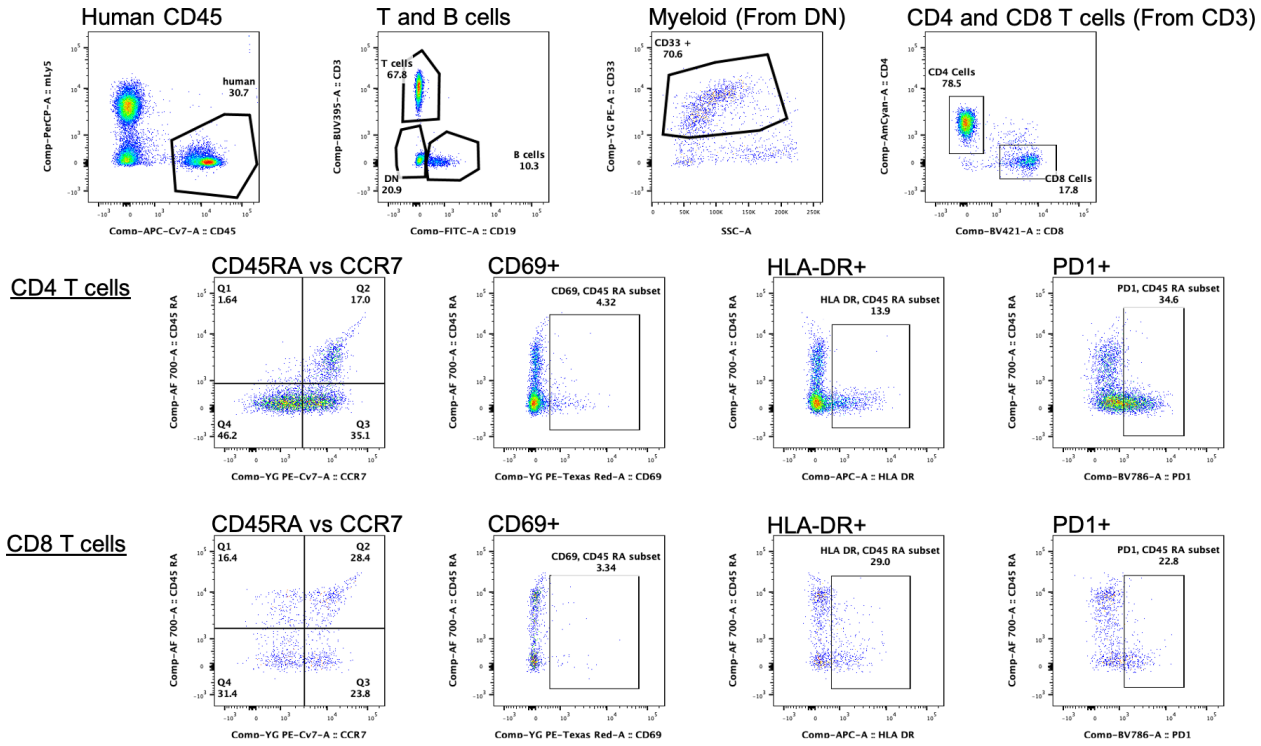

Supplemental Figure S5. Flow cytometry gating scheme for adaptive human immune cell populations isolated from engrafted NSG-SGM3 BLT mice. Flow cytometry analysis gating scheme for human immune cell markers (CD45, general leukocytes; CD19, B cells; CD3, all T cells; CD4, helper T cells (from CD3); CD8, cytotoxic T cells; CD45RA, naïve T cell marker; CCR7, marker for naïve/memory T cells; CD69, T cell activation marker; HLA-DR, T cell activation marker; and PD1, T cell exhaustion marker) analyzed in samples isolated from human immune engrafted NSG-SGM3 BLT mice. Performed two times for blood, spleen, bone marrow, IP lavage, as well as dissociated epididymal fat or cells isolated from the surface of biomaterial implants. N = 5 mice.

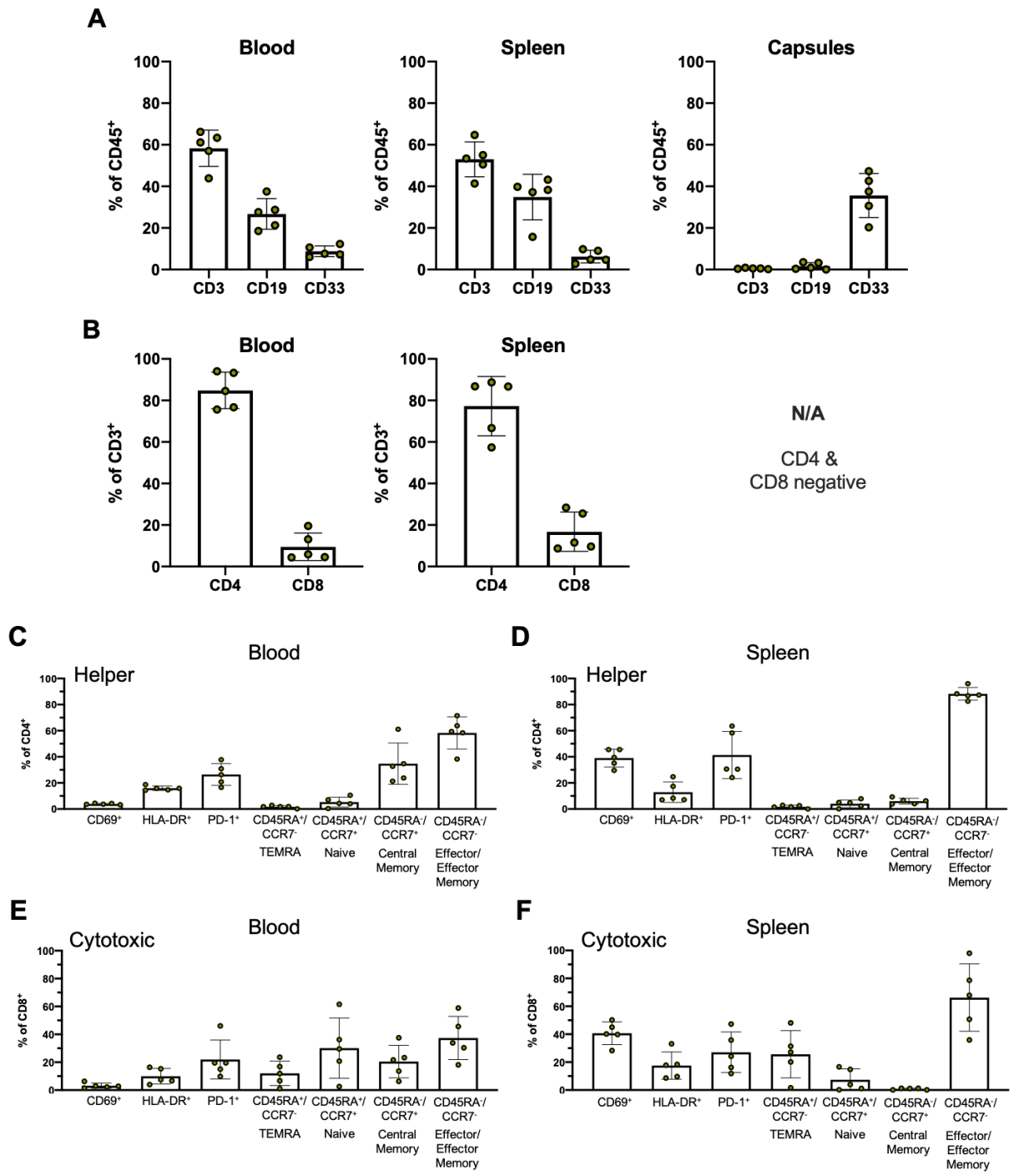

Supplemental Figure S6. Summary of human adaptive immune flow cytometry data for immune cell populations isolated from engrafted NSG-SGM3 BLT mice. A) General human (h) T ($CD3^+$), B ($CD19^+$), and myeloid ($CD33^+CD3^-CD19^-$) subset presence (% of $CD45^+$) in blood (left), in spleen (middle), and on capsules (right). **B**) helper $CD4^+$ T and cytotoxic $CD8^+$ T subsets (% of $CD3^+$) in blood (left), in spleen (middle), and on capsules (N/A, no significant presence and the few $CD3^+$ cells were all $CD4^-CD8^-$). **C-D**) Helper $CD4^+$ T cell subsets (e.g., naïve vs. activated: TEMRA, Central Memory, and Effector/Effector Memory) in blood (left) and spleen (right) taken 2 weeks post-implantation of 500 μm alginate capsules in engrafted NSG-SGM3 BLT mice. **E-F**)

Cytotoxic CD8^{+} T cell subsets (e.g., naïve vs. activated: TEMRA, Central Memory, and Effector/Effector Memory) in blood (left) and spleen (right) taken 2 weeks post-implantation of 500 µm alginate capsules in engrafted NSG-SGM3 BLT mice. Human markers: CD45, general leukocytes; CD19, B cells; CD3, all T cells; CD4, helper T cells (from CD3); CD8, cytotoxic T cells; CD45RA, naïve T cell marker; CCR7, marker for naïve/memory T cells; CD69, T cell activation marker; HLA-DR, T cell activation marker; and PD1, T cell exhaustion marker. Performed two times. N = 5 mice.

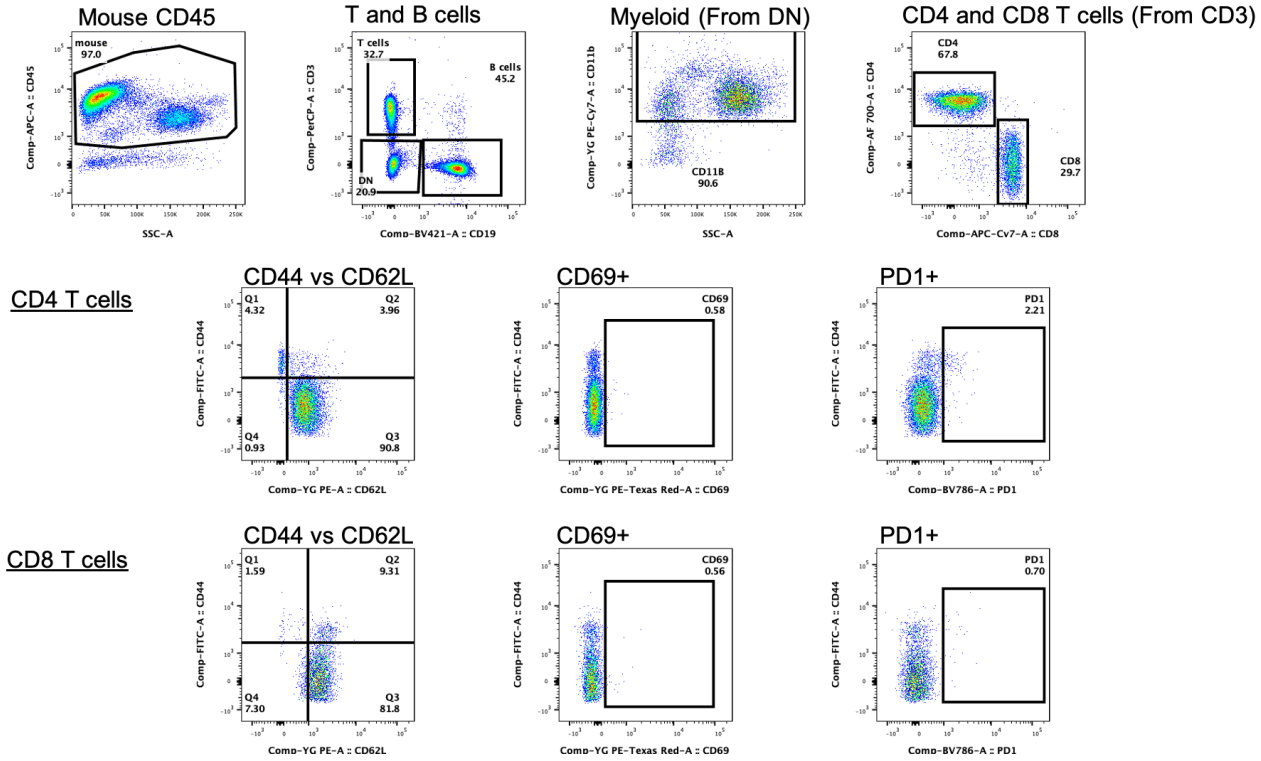

Supplemental Figure S7. Flow cytometry gating scheme for mouse adaptive immune cell populations isolated from wildtype C57BL/6 mice. Flow cytometry analysis gating scheme for human immune cell markers (CD45, general leukocytes; CD19, B cells; CD3, all T cells; CD4, helper T cells (from CD3); CD8, cytotoxic T cells; CD44, lymphocyte activation marker; CD62L, L-selectin on surface of leukocytes; CD69, T cell activation marker; and PD1, T cell exhaustion marker) analyzed in samples isolated from wildtype C57BL/6 mice. Performed two times for blood, spleen, bone marrow, IP lavage, as well as dissociated epididymal fat or cells isolated from the surface of biomaterial implants. N = 5 mice.

A

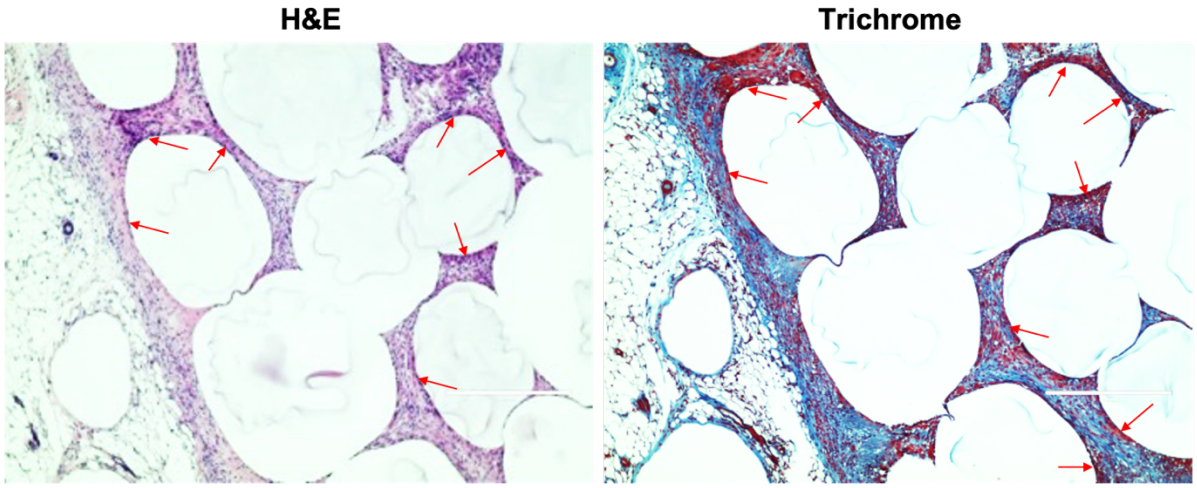

B

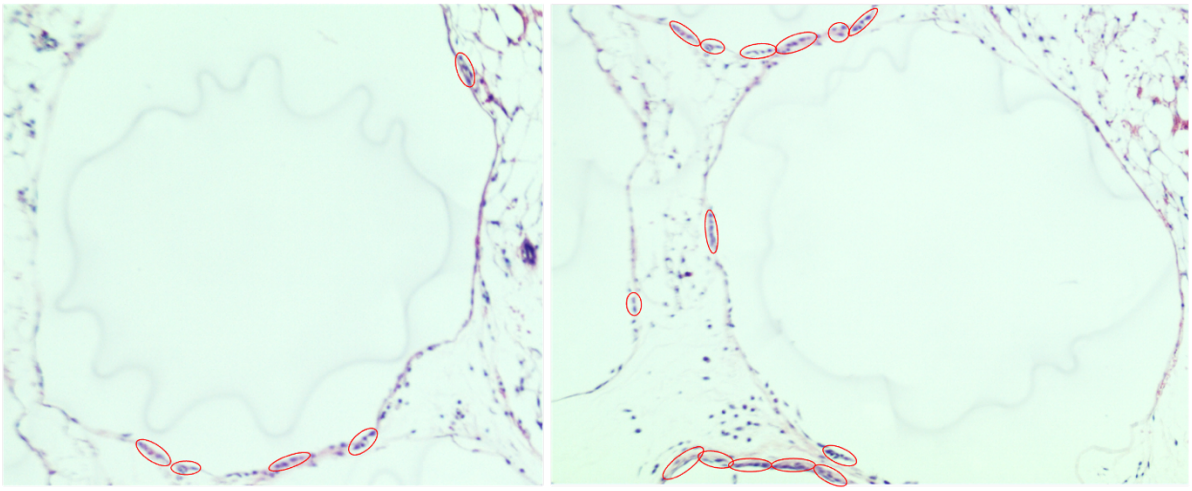

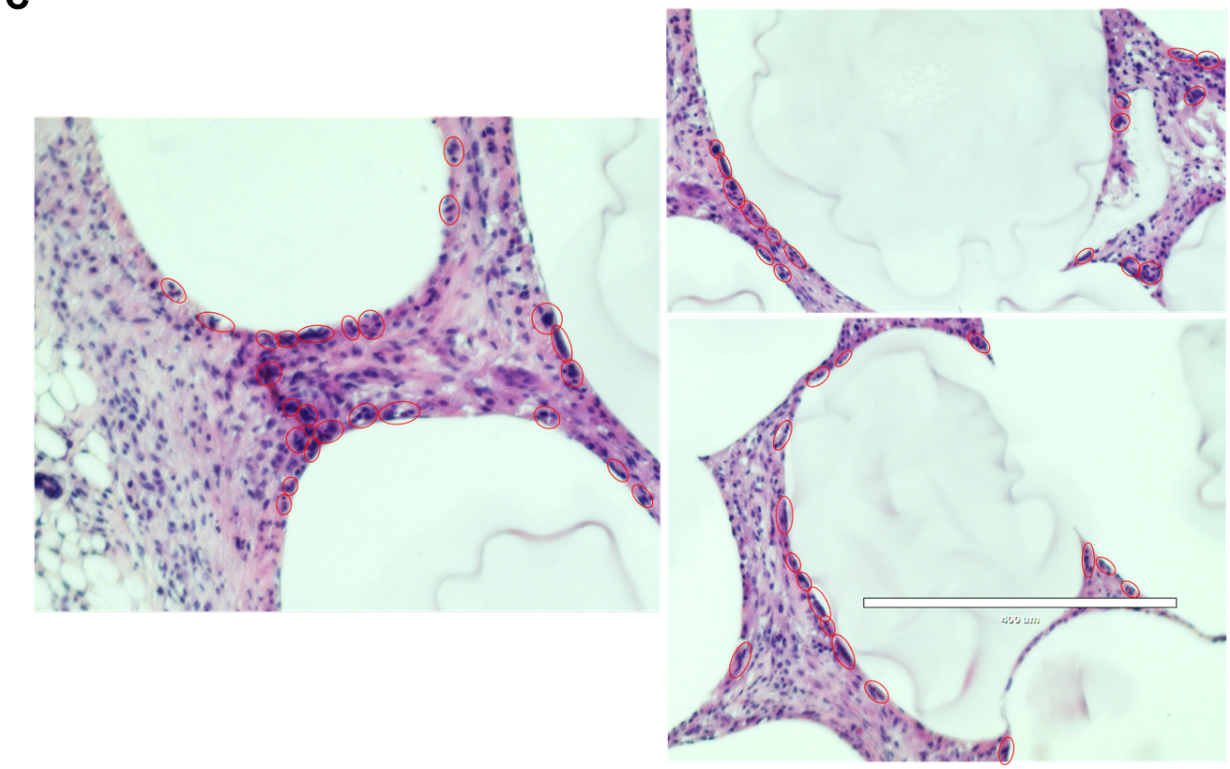

Supplemental Figure S8. Histological analysis showing recapitulated fibrotic & FBGC response in the subcutaneous implant site. A) H&E and Masson's Trichrome staining of fibrotic overgrowth of 500 μm diameter alginate spheres retrieved from the subcutaneous (SC) space of engrafted NSG-SGM3 BLT mice following 4-week implantations (as noted). Magnification, 10X. Higher magnification images of tissues stained for H&E showing FBGC formation as a function of time: **B**) 2 weeks & **C**) 4 weeks post-implantation. Red arrows denote regions of macrophage fusion and foreign body giant cell (FBGC) formation. Magnification, 20X. Images, representative across all mice. Experiment repeated twice.

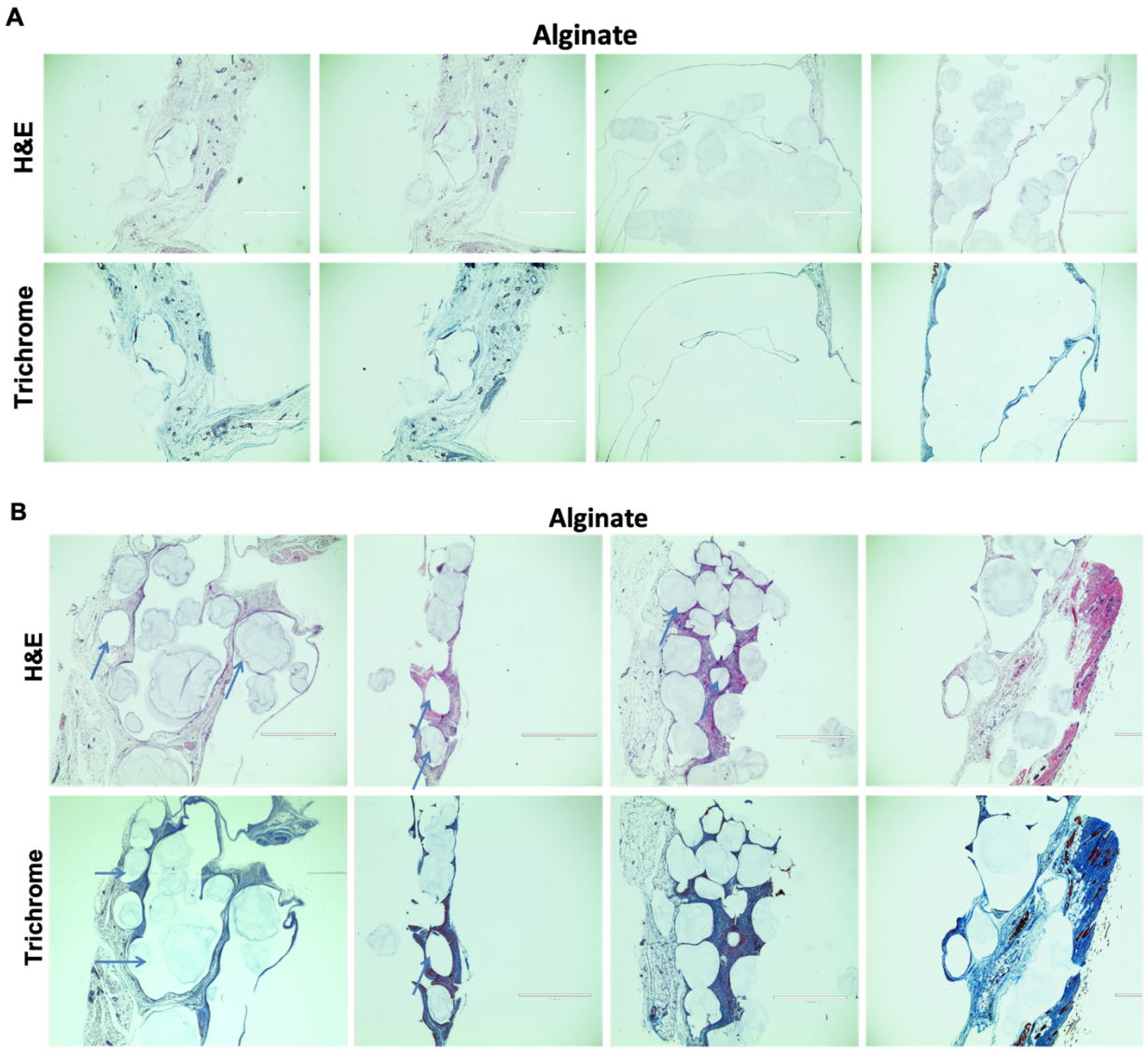
A
Alginate
H&E
Trichrome
B
Alginate
H&E
Trichrome

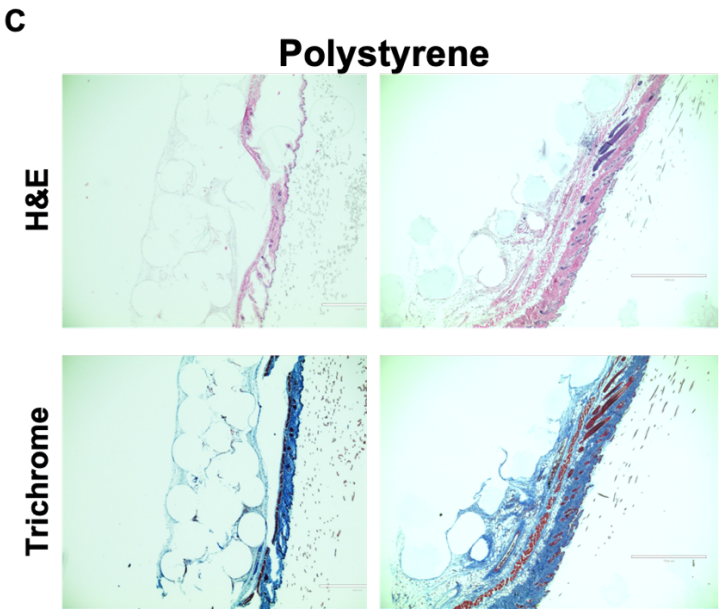

Supplemental Figure S9. **Histological analysis (H&E and Masson's Trichrome) showing developed fibrotic response in the subcutaneous implant site at 2 and 4 weeks. A-B**) 500 μm diameter alginate spheres were retrieved from the subcutaneous (SC) space of human immune engrafted NSG-SGM3 BLT mice following 2 and 4-week implantations, respectively. **C**) 500 μm diameter polystyrene spheres were retrieved from the subcutaneous (SC) space of human immune engrafted NSG-SGM3 BLT mice following 2-week implantations. Images, representative across all mice (n = 5/group); Different magnifications (2X, 4X, and 10X) displayed (as noted). Arrows, pointing to examples of remaining alginate spheres. Experiment repeated twice.

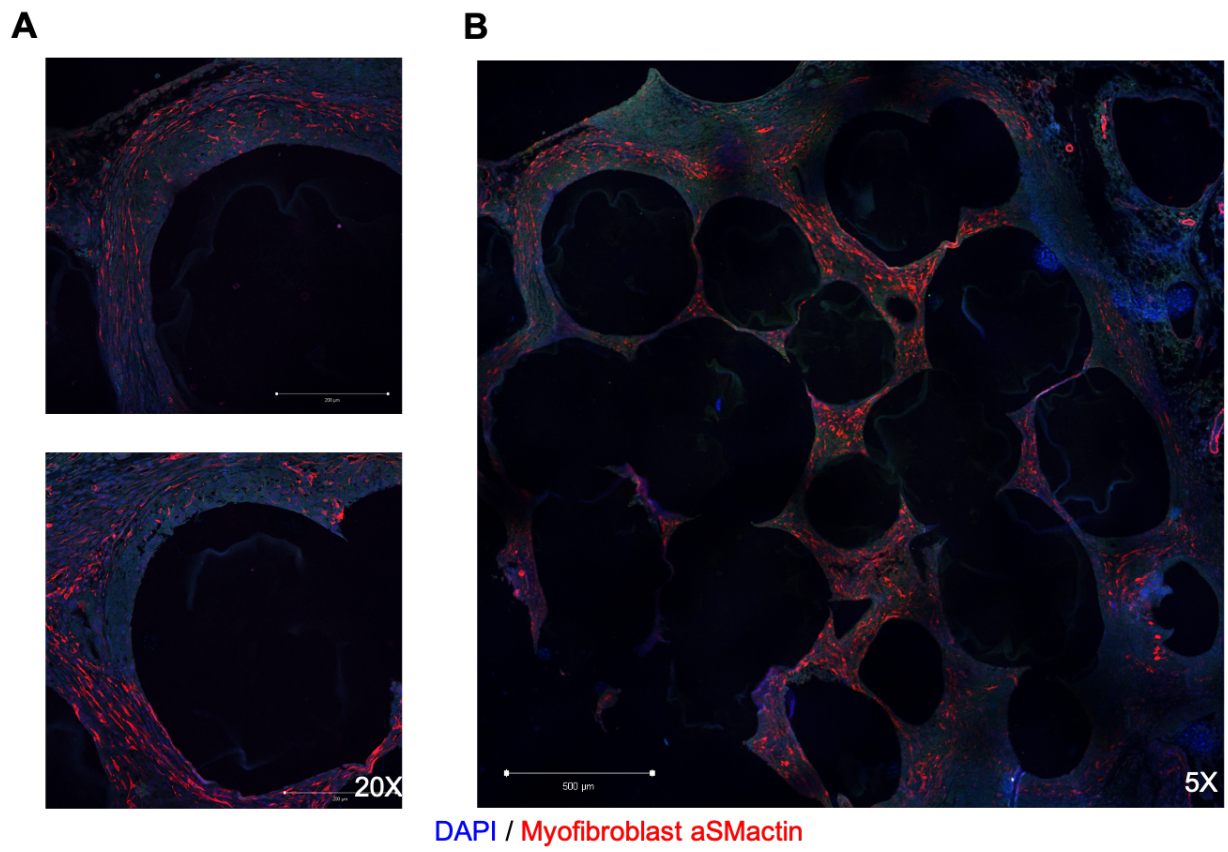

Supplemental Figure S10. Example of immunofluorescence staining of subcutaneous tissue from human immune-engrafted NSG-SGM3 BLT mice. Immunofluorescent images showing cellular nuclei (DAPI, blue), macrophage marker CD68 (green), or myofibroblast marker (alpha Smooth Muscle actin, αSMactin) (red) taken at **A)** high 20X or **B)** low 5X magnification. Experiments performed twice.

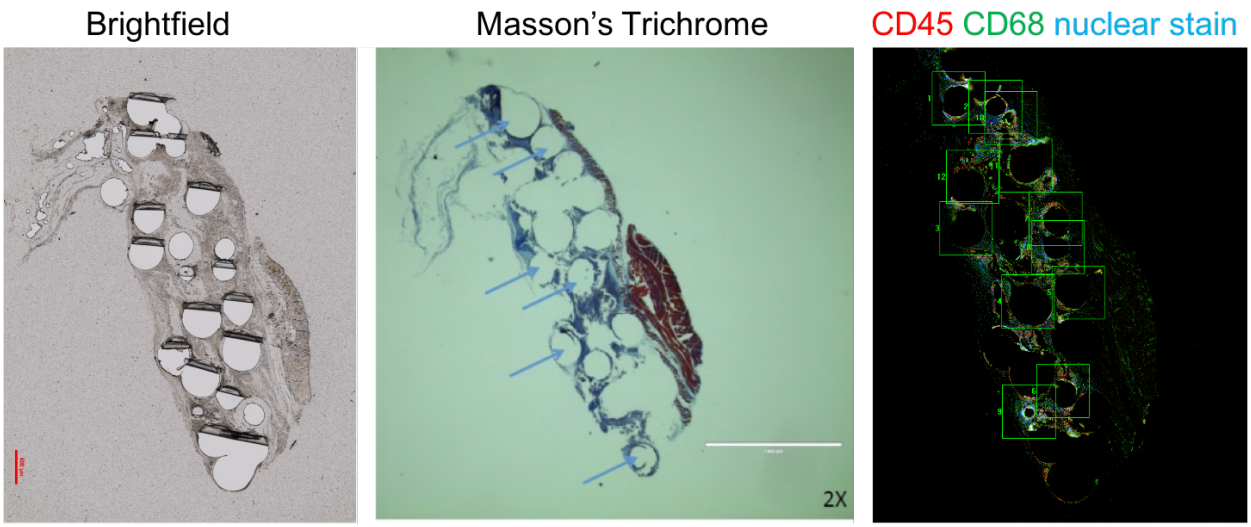

Supplemental Figure S11. Representative brightfield, histology (Masson's Trichrome), and immunofluorescence (IF) panels for subcutaneously implanted polystyrene spheres in engrafted NSG-SGM3 BLT mice. Essential steps in identifying and preparing appropriate positive candidate tissue sections for NanoString's digital spatial profiling (DSP). Samples were first imaged by brightfield, checked by Masson's Trichrome for positive fibrotic encapsulation, and then by IF staining for general immune marker CD45 (red), macrophage marker CD68 (green), and nuclei (DAPI, blue). Once positive candidate areas (green boxes, right image) were identified, up to 20 per sample, DSP analysis using a 30 antibody-multiplexed probe set was used to determine protein dynamics in the tissue immediately surrounding material implants. Representative images from n = 5 mice/group. Experimental analysis run once across n = 2 samples per treatment group (SLG20 and Polystyrene sphere implantation) per time point (2 and 4 weeks), with up to 20 areas of interest (green boxes) per sample.

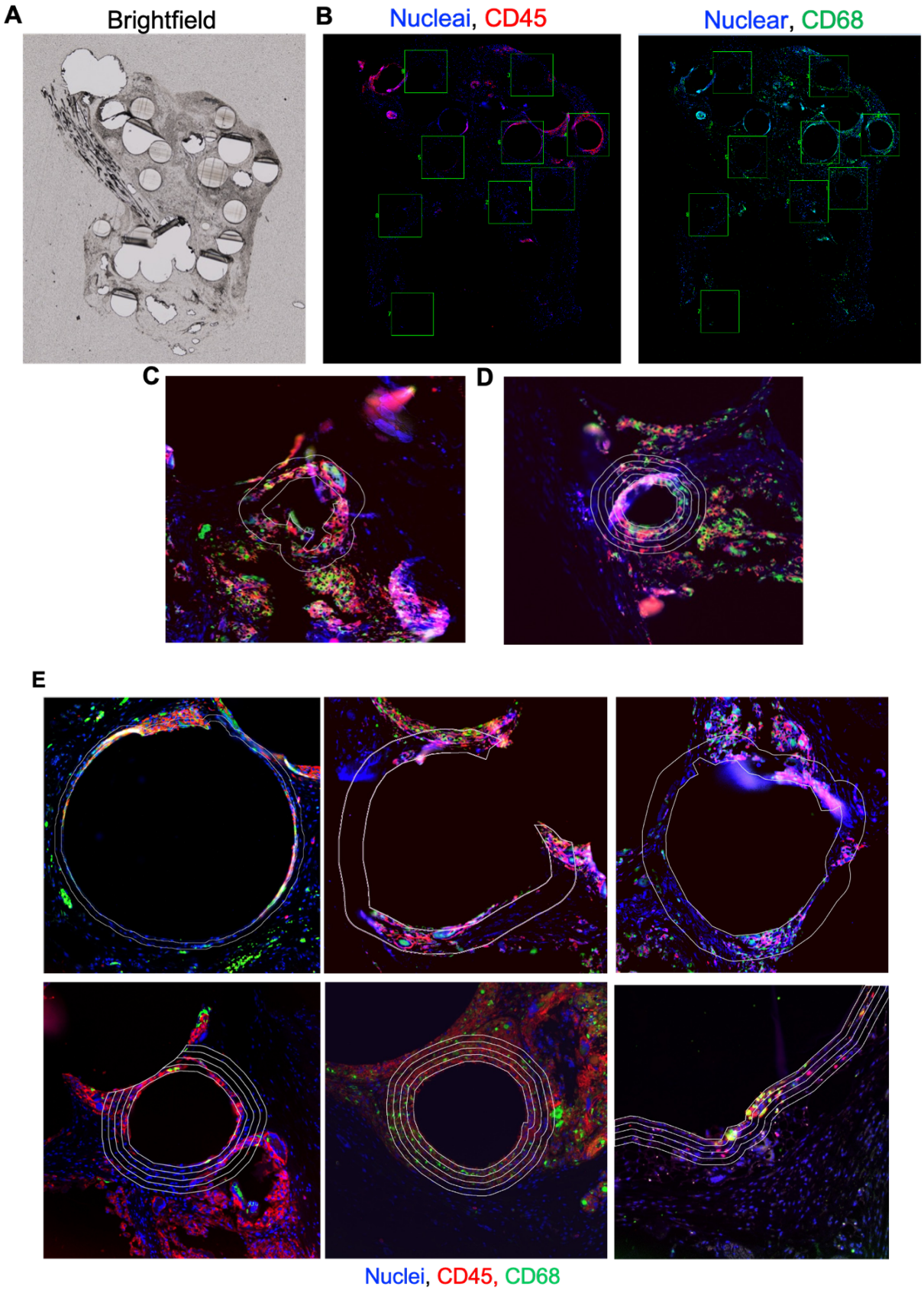
A
Brightfield
B
Nucleai, CD45
Nuclear, CD68
C
D
E
Nuclei, CD45, CD68

Supplemental Figure S12. Additional selection photos for digital spatial profiling (DSP) analysis. Example brightfield **(A)** and immunofluorescence (IF) panels **(B)** for subcutaneously implanted polystyrene spheres in engrafted NSG-SGM3 BLT mice. IF staining: pan-leukocyte immune marker CD45 (red), macrophage marker CD68 (green), and nuclei (DAPI, blue). Once positive candidate areas (green boxes, right image) were identified, up to 20 per sample, DSP analysis using a 30 antibody-multiplexed probe set was used to determine protein dynamics in the tissue immediately surrounding material implants. **C)** Example of one contiguous region of interest (ROI) drawn around one implant sphere for UV ablation and decoupling of nucleotide tags from 30-plex antibody panel. **D)** Example of concentric ring ROIs (multiple) where the UV de-coupling laser was used incrementally in order to isolate antibody probes in 15 µm wedges starting at the material implant-tissue interface and moving outward and away from the implant surface. **E)** Additional examples of expanded lump-sum single ROI vs. concentric ROI-based analyses of immune response in tissue immediately surrounding implanted spheres in fully engrafted NSG-SGM3 BLT mice. Experimental analysis run once across n = 2 samples per treatment group (SLG20 and Polystyrene sphere implantation) per time point (2 and 4 weeks), with up to 20 areas of interest (green boxes) per sample.

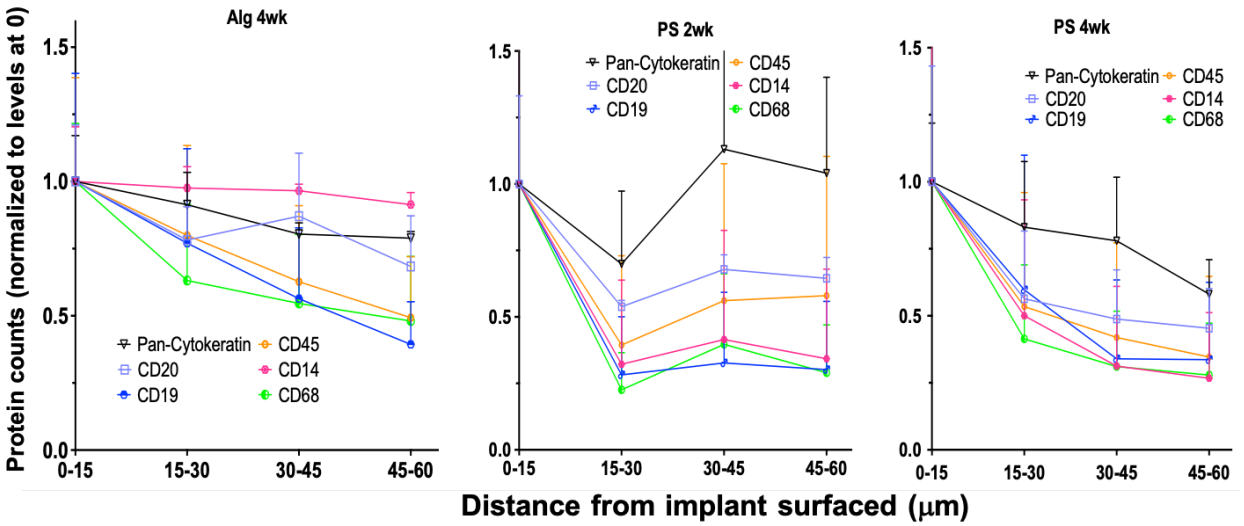

Supplemental Figure S13. Using Digital Spatial Profiling (DSP) to quantify protein levels as a function of distance from implant surfaces. Three line plots (left, middle and right) show quantified protein levels (as denoted) for various immune markers as distance increases away from implant surfaces (in 15 micron concentric rings) for alginate (Alg) (at 2 weeks post-implant) or polystyrene (PS) (2 and 4 weeks post-implant) spheres following subcutaneous retrievals from engrafted humanized NSG-SGM3 BLT mice. Experimental analysis run once across n = 2 samples per treatment group (SLG20 and Polystyrene sphere implantation) per time point (2 and 4 weeks), with up to 20 areas of interest (green boxes) per sample.

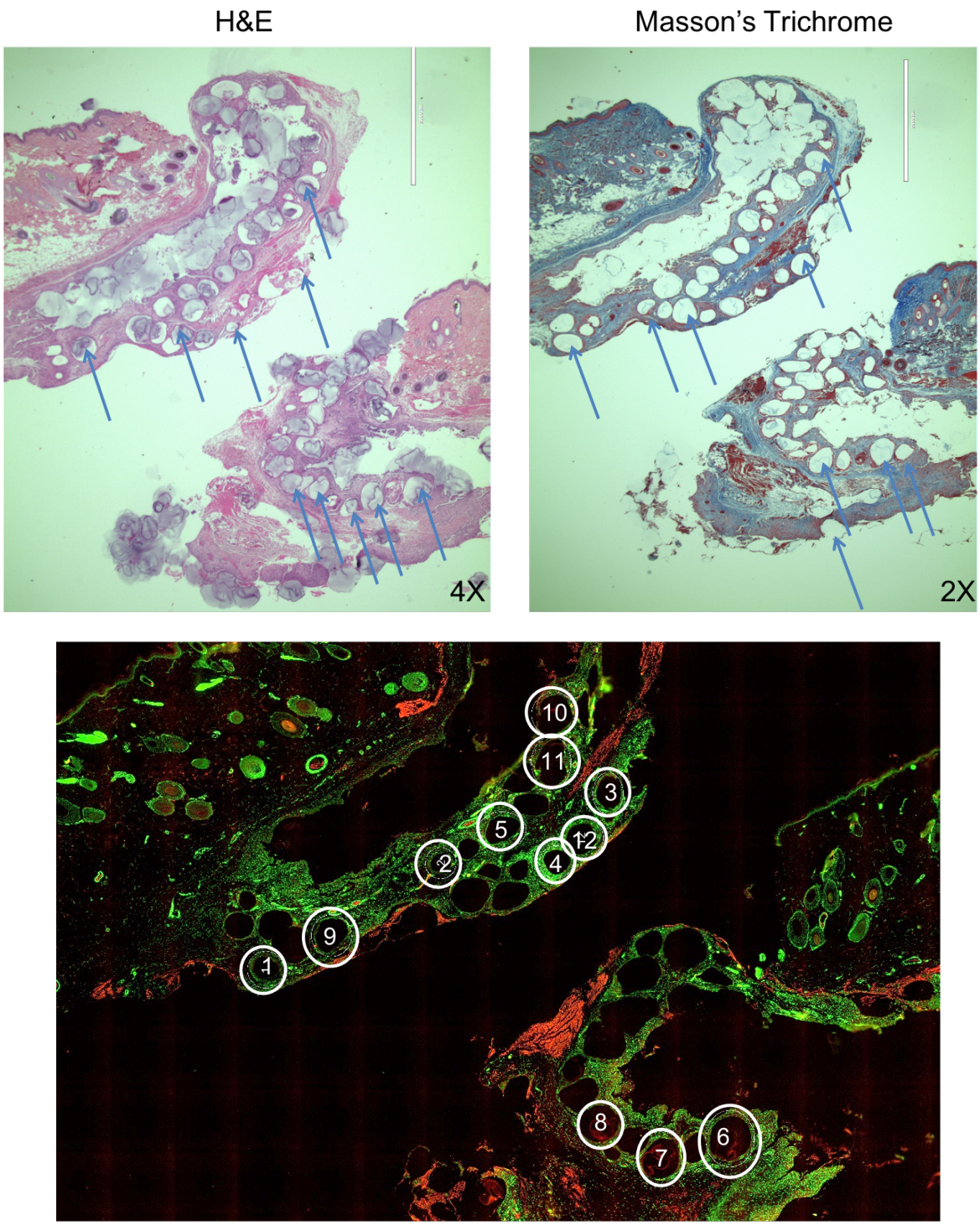

Supplemental Figure S14. Similar DSP setup for tissues from Non-human Primates (NHPs). Essential steps in identifying and preparing appropriate positive candidate tissue sections for NanoString's digital spatial profiling (DSP). Samples were checked by H&E for cellular infiltration and Masson's Trichrome for positive fibrotic encapsulation, respectively, and then by

IF staining for macrophage marker CD68 (red) and alpha Smooth Muscle actin (green). While DSP analysis using a 30 antibody-multiplexed probe set was attempted to determine protein dynamics in the tissue immediately surrounding material implants; unfortunately, the antibodies in the probe set were ultimately not informing for NHP implant response (due to very low signal at the predetermined antibody titrations). Experimental analysis run once across n = 2 NHPs.

2. Supplementary Table:

Table S1. Endotoxin and glucan results for materials utilized in this study. Determined by Charles River Laboratory submission, and in-house testing. E. coli and Limulus Amebocyte Lysates were used as positive controls for general endotoxin. Such negative results have been corroborated previously by our group, and previously published in multiple studies[18-21]. BDL = below detectable limits.

Sample	Endotoxin Test	Glucan Test
Saline control	< 0.05 EU/mL (BDL)	<10 ρg/ml (BDL)
SLG20 alginate 500 μm spheres	< 0.05 EU/mL (BDL)	<10 ρg/ml (BDL)
Polystyrene spheres	< 0.05 EU/mL (BDL)	<10 ρg/ml (BDL)